Antenna design for a cranial implant

Anja K. Skrivervik
Microwave and Antenna Group
Ecole Polytechnique Fédérale de Lausanne
1015 Lausanne, Switzerland
anja.skrivervik@epfl.ch

Alberto Jose Moreno Montes
Microwave and Antenna Group
Ecole Polytechnique Fédérale de Lausanne
1015 Lausanne, Switzerland

Ismael Vico Trivino
Microwave and Antenna Group
Ecole Polytechnique Fédérale de Lausanne
1015 Lausanne, Switzerland
ismael.vicotrivino@epfl.ch

Marko Bosiljevac
Faculty of Electrical Engineering and Computing
University of Zagreb
Zagreb, Croatia
marko.bosiljevac@fer.hr

Miroslav Veljovic
Microwave and Antenna Group
Ecole Polytechnique Fédérale de Lausanne
1015 Lausanne, Switzerland
miroslav.veljovic@epfl.ch

Zvonimir Sipus
Faculty of Electrical Engineering and Computing
University of Zagreb
Zagreb, Croatia
zvonimir.sipus@fer.hr

***Abstract*—This contributions presents the design process for an antenna designated for the telemetry in a cranial implant. Issues like physical limitation, simulation problems and design strategies will be addressed and final design presented.**

Keywords—implantable antenna, design strategy

I. Introduction

The number of application for implantable sensors has increased rapidly over the past years, medical implants taking a significant share of this increase [1-4]. These implants need to communicate wirelessly with base stations or nodes located outside the host body, and thus require heavily miniaturized and integrated antennas. There exists an increasing demand for miniature antennas suitable to be integrated in these implants. There are many examples of antennas for implants or ingestibles available in literature (non-exhaustive examples given in [4-9]). However, establishing efficient links with implants remains a major challenge due to the losses in the body hosting the implant. In order to achieve acceptable links and minimize the losses, a new design needs to be done for each new application and situation. Thus, efficient design strategies are required.

In this contribution, we present the design of an antenna for a cranial implant, illustrating different steps and pitfalls inherent to such a design. In section II, the design requirements will be presented, followed by the design procedure in section III. The system will be presented in section IV.

II. Requirements

The design requirements are as follows: The implant is placed in the scull of the human head (bone layer) behind the ear. It will communicate with a wearable node placed close to the skin. The dimensions allotted to the implanted antenna, including a biocompatible insulation layer is 8 x 8 x 2 mm^3. The biocompatible layer can either have a low dielectric permittivity (e.g. PEEK, with ε_r=3.2, tan δ=0.01) or a high dielectric permittivity (e.g. Zirconia with ε_r=29, tan δ=0.002). Frequency of operation is 5.8 GHz and the losses between the implanted and wearable nodes should be less than 50 dB over a 100 MHz frequency band. The wearable node will use a simple microstrip patch antenna. The latter will be covered by a PEEK spacer that will be in direct contact to the skin of the user.

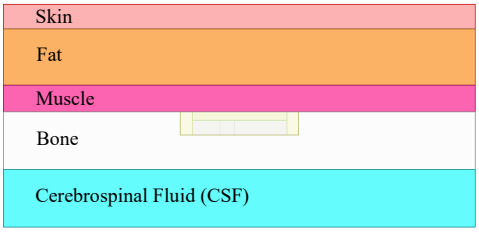

Fig. 1. Phantom used in the design phase, with the position of the implant in pale yellow.

TABLE I. Characteristics of the Head Phantom

	h (mm)	ε_r	tanδ
Skin	2.2	35.1	0.33
Fat	4.8	9.9	0.26
Muscle	2.4	48.48	0.32
Bone	5	9.7	0.37
CSF	5	60.47	0.40

III. Design

The phantom used for the design of the antenna is depicted in Fig. 1. The nominal thickness and dielectric characteristics [10] of the layers are given in Table I. The real thickness of those layer can vary greatly form subject to subject, thus the robustness of the link should be checked versus variations of those values.

Before starting with the design, we checked the feasibility of the link by analyzing a simpler canonical problem using the techniques described in [11, 12]. In this analysis, we study the attenuation of the power density transmitted by an elementary source (Hertzian electric dipole) located in a spherical phantom, having a radius of 10 cm and where the outer layers are the same bone, fat and skin layers as in our phantom. This model is depicted in Fig. 2, with an electric Hertzian dipole placed at the center of an air bubble of a 2-mm radius located in the bone layer flush to the muscle layer. The radiation of this source is computed using a spherical wave expansion, which has the advantage of being very fast to solve numerically. The result of this check is depicted in Fig. 3, where we see the decrease of the power density computed on a radial line from the source to free space.

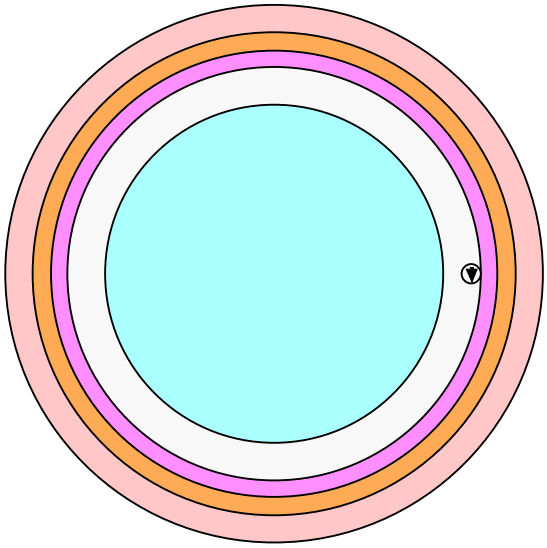

Fig. 2. Spherical model used for the feasibilty analysis. The arrow represents an electric Hertzian dipole, located in an air encapsulation, placed in the bone layer.

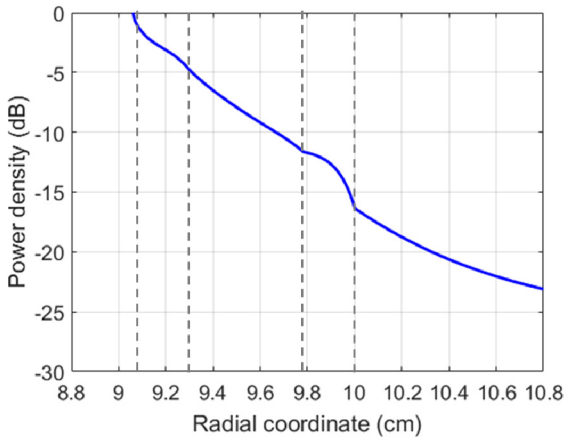

Fig. 3. Power density on a radial line from the source to the free space, computed using a spherical wave expansion.

The path loss in the case of an elementary model is around 25 dB. This result, albeit obtained for a simplified model, indicates that our link is feasible as it leaves a margin of 25 dB between the simplified canonical model and the requirements.

Due to the antenna dimension defined in the requirements, a PIFA placed in a cavity is a good candidate for an initial design. The substrate used is Rogers TMM10i (ε_r=9.8 and tanδ =0.002). Two cases are considered, a PIFA covered by a low-permittivity insulator and a PIFA covered by a high-permittivity insulator.

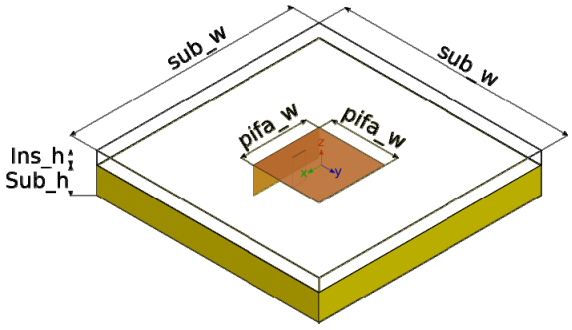

(a) PIFA and insulator parameters.

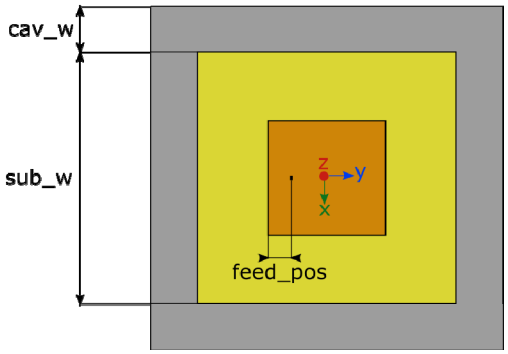

(b) Feeding and cavity parameters.

Fig. 4. Final design of the cavity-backed PIFA. Dimensions are given in Table II.

The antenna is depicted in Fig. 4, while the dimensions for both cases are given in Table II. Both antennas cover the bandwidth required, as the -10 dB bandwidth for the PEEK-covered antenna is 360 MHz and the bandwidth for the Zirconia-covered antenna is 450 MHz. In order to select the best option between the two antennas, we compared their performance in the real phantom (Fig. 1), and in simplified phantoms made of muscle only, and of lossless muscle only. The results are shown in Figs. 5 and 6 for the two covering materials. We see that the reflection of the Zirconia-covered antenna is more sensitive to the presence of the losses in the tissues surrounding it, which lead us to select the PEEK covered antenna as a better solution.

IV. System Results

In order to characterize the link losses between the implanted and the wearable nodes, the phantom described in Fig. 7 was used, with the same layers as before. The wearable node antenna is a simple cavity-backed patch antenna printed on PEEK and covered by PEEK, as a biocompatible layer is in contact with the skin of the user.

TABLE II. Dimensions of Final Antennas in mm

Cover Material	pifa_w	feed_pos	sub_h	ins_h	sub_w	cav_w
PEEK	3.3	1.24	1.27	0.73	8	10
Zirconia	0.75	0.1	1.27	0.73	8	10

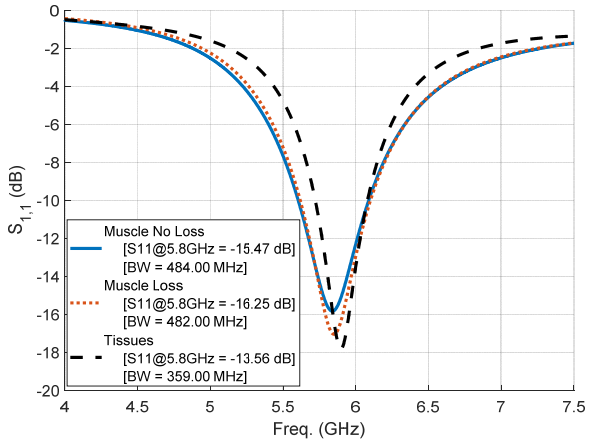

Fig. 5. Reflection coefficient for the PEEK-covered antenna surrounded by an homogeneous muscle phantom, with or without losses, and by the final multilayered phantom

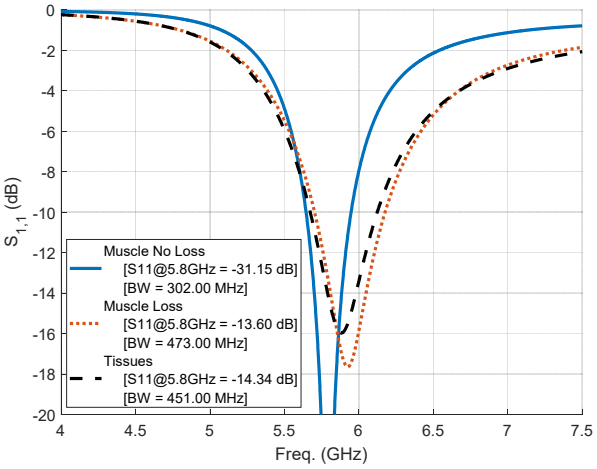

Fig. 6. Reflection coefficient for the Zirconia-covered antenna surrounded by an homogeneous muscle phantom, with or without losses, and by the final multilayered phantom.

It has to be noted that, due to significant change in permittivity between the layers, a part of the power radiated by the implanted PIFA is reflected at the dielectric boundaries and guided laterally inside the tissues. This is illustrated in Fig. 7, where the magnitude of the E field is plotted for different transverse dimensions of the phantom. In the simulations, the phantom is terminated laterally by perfect absorbing boundaries.

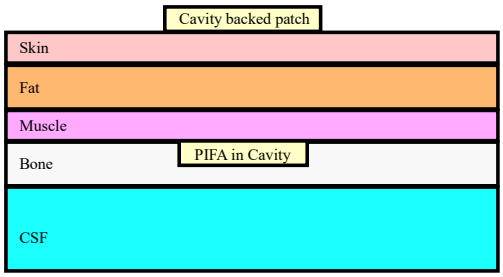

Fig. 7. Phantom for the transmission between wearable and implanted nodes.

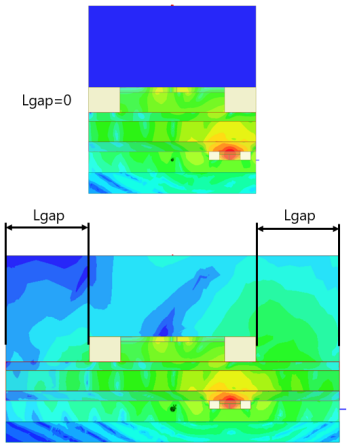

Fig. 8. E field distribution through the antennas and the phantom for different phantom sizes.

The purpose of the cavity, in the implanted PIFA, is to minimize the effect of the lateral guiding of the waves. The vertical walls of the cavity serve to block this lateral propagation, and focus the radiation in the broadside direction, towards the wearable node. This effect is more significant for the PEEK-covered PIFA, as the difference in permittivity is larger, compared to the surrounding tissue.

However, the transmission between the nodes is not affected by the size of the phantom, as is demonstrated in Fig. 9 and 10. This comes from the high losses in the tissues. Thus, in order to accelerate the simulation time, it is sufficient to use a small phantom. Finally, the transmission coefficient between the wearable and implanted nodes was also simulated using the Zirconia-covered PIFA for the implant. In this case, the results were 10 dB worse than for the case of the PEEK-covered PIFA. This worse behavior was expected from our analysis of the sensitivity of the antennas to the losses in the tissues surrounding the implant.

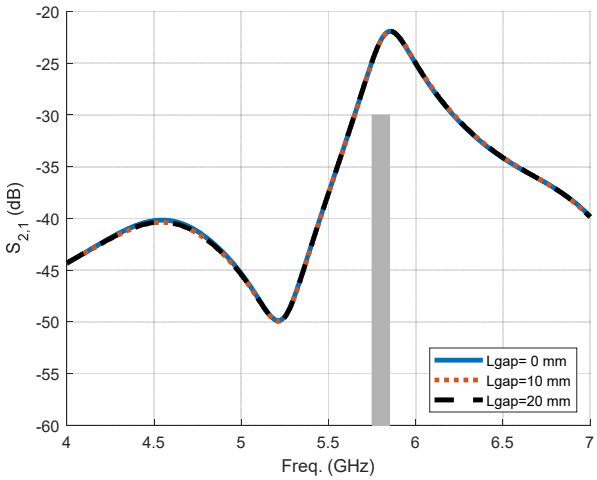

Fig. 9. Transmission between the wearable and implanted antenna with PEEK insulator for different phantom sizes.

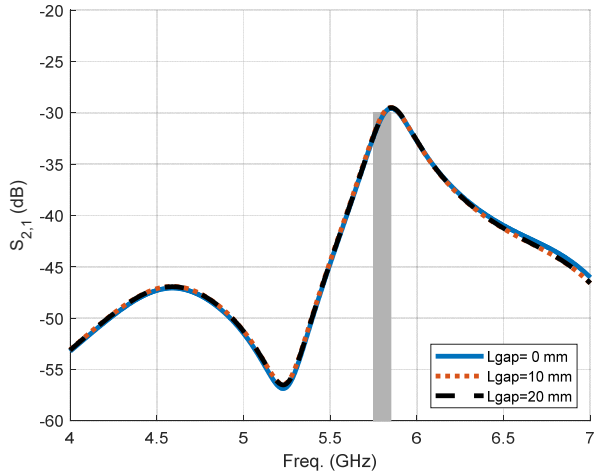

Fig. 10. Transmission between the wearable and implanted antenna with Zirconia insulator for different phantom sizes.

V. Summary

The design of an antenna for a cranial implant has been presented, and the transmission between the implant and a wearable node analyzed. In line with the requirements, a transmission coefficient better than -30 dB over the requested bandwidth was achieved. It is noticeable that this result closely matches the results foreseen using a simplified model, which indicates the usefulness of such approaches to assess the feasibility of a link prior to investing time simulating a more accurate model. In-vitro measurements will be presented at the conference.

References

[1] E. Katz, Implantable Bioelectronics. Weinheim, Germany: Wiley, 2014.

[2] D. Nikolayev, M. Zhadobov, R. Sauleau, and P. Karban, “Antennasfor ingestible capsule telemetry,” in Advances in Body-Centric Wireless Communication: Applications and State-of-the-Art, London, UK: IET, 2016, pp. 143–186.

[3] A. Kiourti and K. S. Nikita, “A review of in-body biotelemetry devices: implantables, ingestibles, and injectables,” IEEE Trans. Biomed. Eng., vol. 64, no. 7, pp. 1422–1430, Jul. 2017.

[4] F. Merli, L. Bolomey, J.-F. Zürcher, G. Corradini, E. Meurville and A.K. Skrivervik, Design, realization and measurements of a miniature antenna for implantable wireless communication systems, IEEE Transactions on Antennas and Propagation, , vol. 59, issue 10, 2011, pp. 2544-2555

[5] Z. Jiang et al., “Wideband loop antenna with split ring resonators for wireless medical telemetry,” IEEE Antenn. Wireless Propag. Lett., vol. 18, no. 7, pp. 1415–1419, Jul. 2019

[6] W. Lei and Y. Guo, “Design of a dual-polarized wideband conformal loop antenna for capsule endoscopy systems,” IEEE Trans. Antennas Propag., vol. 66, no. 11, pp. 5706–5715, Nov. 2018.

[7] Z. Bao, Y.-X. Guo, and R. Mittra, “Conformal capsule antenna with reconfigurableradiation pattern for robust communications,” IEEE Trans. Antennas Propag., vol. 66, no. 7, pp. 3354–3365, Apr. 2018

[8] D. Nikolayev, M. Zhadobov, L. Le Coq, P. Karban, and R. Sauleau,“Robust ultra-miniature capsule antenna for ingestible and implantable applications,” IEEE Trans. Antennas Propag., vol. 65, no. 11, pp. 6107–6119, Nov. 2017

[9] M. K. Magill, G. A. Conway, and W. G. Scanlon, “Tissue-independent implantable antenna for in-body communications at 2.36–2.5 GHz,”IEEE Trans. Antennas Propag., vol. 65, no. 9, pp. 4406–4417, Sep. 2017.

[10] M. Ackermann, "the visble human project", Proc. IEEE, vol. 86, No 3,1998, pp. 504-511.

[11] Anja K Skrivervik, Marko Bosiljevac, Zvonimir Sipus, "Fundamental Limits for Implanted Antennas: Maximum Power Density Reaching Free Space", IEEE Trans. on Antennas and Propagation, Vol. 68, No8, 2019, pp. 4978 – 4988.

[12] M. Bosiljevac, Z. Sipus, A.K. Skrivervik, "Propagation in Finite Lossy Media: an Application to WBAN", Antennas and Wireless Propagation Letters, IEEE, Year: 2015, Volume: 14, PP 1546 – 1549.